energies

MDPI

Article

Organic Supercritical Thermodynamic Cycles with Isothermal Turbine

Marian Piwowarski *, Krzysztof Kosowski and Marcin Richert

Faculty of Mechanical Engineering, Gdansk University of Technology, Gabriela Narutowicza Street 11/12, 80233 Gdansk, Poland; krzysztof.kosowski@pg.edu.pl (K.K.); marrich1@student.pg.edu.pl (M.R.)
* Correspondence: marian.piwowarski@pg.edu.pl; Tel.: +48-58-347-14-29

Abstract: Organic Rankine cycles (ORC) are quite popular, but the overall efficiencies of these plants are rather very low. Numerous studies have been conducted in many scientific centers and research centers to improve the efficiency of such cycles. The research concerns both the modification of the cycle and the increase in the parameters of the medium at the inlet to the turbine. However, the efficiency of even these modified cycles rarely exceeds 20%. The plant modifications and the optimization of the working medium parameters, as a rule, lead to cycles with the high pressure and high temperature of live vapor and with a regenerator (heat exchanger) for the heating, vaporization and superheating of the medium. A new modified cycle with supercritical parameters of the working medium and with a new type of turbine has been described and calculated in the paper. For the first time, the isothermal turbine is proposed for supercritical organic cycles, though this solution is known as the Ericsson cycle for gas turbines. The innovative cycle and the usual ORC plants are characterized by almost identical block diagrams, while in the proposed cycle, the work of the turbine is obtained as a result of isothermal expansion and not in an adiabatic process. The analysis has been performed for 11 different working media and two cycles. The calculations have shown that power plants with isothermal expansion achieve better efficiency than cycles with adiabatic turbines. For example, the rise in efficiency changes from 8 percentage points for R245fa up to 10 percentage points for acetone. The calculations have proved that it is possible to obtain efficiency exceeding 50% for organic power plants. This is an outstanding result compared with modern steam and gas turbine units.

Keywords: supercritical thermodynamic cycles; organic media; efficiency; isothermal expansion; adiabatic expansion

Citation: Piwowarski, M.; Kosowski, K.; Richert, M. Organic Supercritical Thermodynamic Cycles with Isothermal Turbine. *Energies* **2023**, *16*, 4745. https://doi.org/10.3390/en16124745

Academic Editors: Andrea De Pascale and Fabio Polonara

Received: 31 March 2023
Revised: 4 June 2023
Accepted: 14 June 2023
Published: 15 June 2023

1. Introduction

The idea of ORC systems was born relatively long ago; the first systems were built in the 1960s. It is a variation of the steam cycle called the organic Rankine cycle (ORC). This name refers to steam cycles in which organic compounds are used as a working medium. They can be various fluids, ranging from short aliphatic hydrocarbons, through aromatic compounds, to complex synthetic freons. As for the components of ORC installations, they do not differ from standard steam systems (pump, steam generator, turbine, condenser). Initially, these power plants were installed mainly in the USA, Japan, Germany, Israel and Italy and reached power from several dozen kilowatts to several megawatts. Typical refrigerants used at the time were toluene, R11, R12, R113, R114 and Florinol [1]. A characteristic feature of these systems is the ability to operate at lower temperatures than is possible with water. They can also operate in a different pressure range, for example, condensing at atmospheric pressure. Very often, the top source of energy in ORC cycles is waste heat from various energy, agricultural or domestic processes [2,3]. You can find the use of waste heat from technological processes in industrial facilities (e.g., metallurgical, cement, etc.) [4,5]. In the literature on the subject, there are numerous cases of using

the heat emitted by internal combustion engines [6] and gas turbines [7] in these power plants. Thanks to such applications, it is possible to increase the overall efficiency of the existing gyms by several percentage points. Some frequently analyzed heat sources for ORC systems are geothermal energy [8] and solar energy [9]. There are also examples of using the thermal energy of the oceans as a source of heat for ORC power plants [10]. Fluids working in ORC power plants should meet a number of requirements not related to thermodynamic properties. First of all, they should not be toxic substances and should be environmentally friendly. They should be cheap and easily accessible. They cannot react with the elements of the flow system. Often, not all of these conditions can be met while maintaining good thermodynamic properties. This results in the necessity to build better-secured and thus more expensive installations. This is the case, for example, when using combustible gases as working media. A big challenge for designers is choosing the right working medium. The literature on the subject contains a large number of fluids that can be used in ORC cycles. Saturated, unsaturated hydrocarbons, cyclic, heterocyclic, aromatic, various refrigerants, alcohols, siloxanes and others are considered. Many mixtures and their thermodynamic properties are not commercially available, and some of them are protected by patents. A well-matched organic medium should, above all, enable the system to operate with the highest possible efficiency and make it possible to significantly utilize the available heat source. In the literature on the subject, as a rule, several factors are analyzed as working fluids in ORC systems, incl. R245fa, R123, n-butane, n-pentane, R1234yf [11] ethanol [12], R134a, R152a, R236fa, R245fa, R404a SES36 [13], toluene, siloxanes [14], ammonia, cyclohexanes or acetone [15]. Power plants with organic Rankine cycles (ORC) differ significantly in efficiency from systems in which water is used, mainly due to the very low temperature in front of the turbine. As a result, these installations achieve an efficiency of about 10%, and only exceptionally can they reach about 20% thanks to the use of various modifications [16]. It is possible to increase the efficiency of the cycle by increasing the upper temperature [17] and modifying the installation structure, e.g., by adding an additional cycle [18] or by using an additional heater [19]. As in the case of steam turbines, efficiency can be increased by using an inter-stage superheater [20], regenerators [21,22] or by using a parallel evaporator [23]. Sometimes the efficiency of power plant components such as turbines, compressors, boilers, pumps and electric generators can also be improved. Although there are certain limitations (material strength, technology), the efficiency of some power plant components is very impressive, e.g., the internal efficiency of modern gas turbines [24] or the most advanced medium-pressure steam turbines can reach 93–94% [25]. There are intensive efforts to find better solutions in order to develop new types of power plants and new cycles. An important element determining and classifying ORC power plants, apart from the temperature of the source from which the heat is taken, is the operating pressure of the cycle. A review of the literature showed that the efficiency of even the most complex ORC systems is low compared to other solutions used in the power industry. Currently, very intensive works are underway to increase the efficiency of the ORC power plant by increasing the parameters of the working medium [26,27].

However, we suggest an innovative cycle of significantly better efficiency. The proposed cycle and the ORC are represented by the same block diagram, Figure 1a. In the case of a typical ORC, an adiabatic turbine is in use, Figure 1b. In the new cycle, an isothermal turbine is applied. The interpretation of this cycle in the temperature−entropy diagram is shown in Figure 1c. In this cycle, heat is added during the vapor generation (q_{1a}) and during the isothermal expansion (q_{1b}) while heat is rejected in the condenser (q_2). Work is generated in the isothermal turbine, and only a relatively small amount of it is used for the pump. In the regenerator, the superheat of the steam coming from the turbine after the isothermal expansion is used for the heating, evaporation and superheating of the medium. In turn, heat is supplied to the steam generator to further superheat the medium at the turbine inlet. In order to reach the final live vapor temperature, some heat q_{1a} from external sources is added. In the turbine, heat q_{1b} is introduced to realize the isothermal expansion. In this way, the proposed cycle is very similar to the Ericsson cycle known as

the generalized Carnot cycle. The authors propose a new organic cycle which leads to a rise in efficiency up to 10 percentage points in the calculated variants (in the same temperature range). A new isothermal turbine is applied in the power plants which may be treated as the most important innovation.

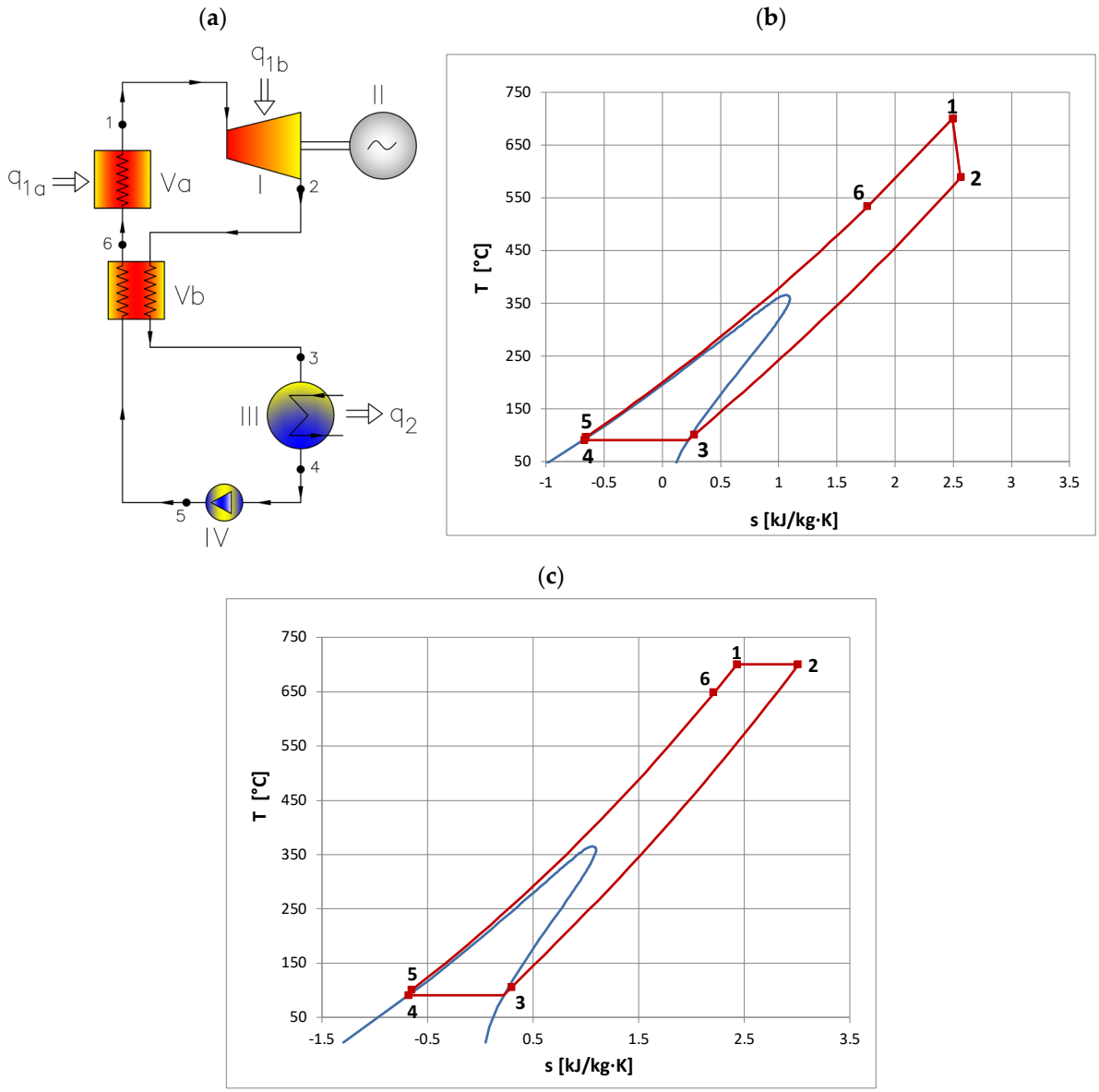

Figure 1. Supercritical organic cycle for dry fluids (**a**), interpretation in temperature−entropy diagram for ORC with adiabatic expansion (**b**), interpretation in temperature–entropy diagram for cycle with isothermal expansion (**c**); where: I−turbine, II−electric generator, III−condenser, IV−main pump, Va−vapor generator, Vb−regenerator q_{1a}−heat delivered to the vapor generator, q_{1b}−heat delivered during isothermal expansion, q_2−heat rejected with the water cooling condenser, blue curve−limit line, red line− calculated cycle, digits from 1 to 6 are the characteristic points of the analyzed cycle, according to the markings in Figure 1a.

The calculations showed that thanks to the use of an isothermal turbine and increasing the parameters of the working medium, it is possible to design an ORC power plant with efficiency comparable to modern steam turbines. In addition, at the end of the work, there is an example showing how to carry out isothermal expansion for one of the fluids analyzed in the study (Appendix A). These types of power plants seem to be a new approach that has not been considered and described so far. However, in the bibliography,

some thermodynamic cycles with near-isothermal expansion have been described, both for turbines [28] as well as piston machinery [29]. Those methods consisted of injecting streams of hot medium into the main flow, but the effectiveness of this approach is uncertain. There are also no other mentions in the literature on this subject.

2. Modelling

The cycle diagram is the same for all the analyzed variants, but the plants vary in the type of expansion in the turbine. In both, the cycles live vapor is obtained in a vapor generator in which the heat of superheating is used for the heating, vaporization and superheating of the medium as well as the heat from an external resource.

The analysis includes two variants of power plants with different turbines:

Variant 1: cycle with adiabatic expansion in the turbine (AD);

Variant 2: cycle with the isothermal turbine (IZT).

Each cycle has been analyzed with the adiabatic (AD) and isothermal (IZT) turbines, so two variants of the cycle have been considered for each fluid.

The calculations have been performed assuming the upper and lower parameters of the working medium. The properties of the working fluids have been determined using the REFPROP [30] media library. Standard thermodynamics formulae have been used, occasionally applying the iteration method (when values of specific heat, which depend on other thermodynamic parameters, have been calculated). The basic equations are presented below:

- heat delivered to the working media between the regenerator and the turbine nozzles:

$$q_{1a} = (i_1 - i_6), \tag{1}$$

where:

q—heat,
i—enthalpy,
indexes refer to points marked in the diagram (Figure 1),

- heat of the isothermal expansion

$$q_{1b} = T_1 \cdot \Delta s = T_1 \cdot (s_2 - s_1), \tag{2}$$

T—temperature,
s—entropy,
Δ—gradient,

- heat rejected in the condenser:

$$q_2 = (i_3 - i_4), \tag{3}$$

- adiabatic turbine work:

$$l_{T\_AD} = (i_1 - i_2), \tag{4}$$

l—work,

- isothermal turbine work:

$$l_{T\_IZT} = T_1 \cdot \Delta s + \Delta i = T_1 \cdot (s_2 - s_1) + (i_1 - i_2), \tag{5}$$

- pump work:

$$l_{PG} = (i_5 - i_4). \tag{6}$$

Energy efficiency is understood as the relation between the net electric power and the heat flux supplied to the plant, given by the equation:

$$\eta_{el} = \frac{N_{el}}{\dot{Q}_D}, \tag{7}$$

N − power,

$\dot{Q}_D$ − heat flux.

Depending on the variant, the net electric power is the power obtained in the turbine N_T, diminished by the power N_{PG}, used to drive the pump and by the losses in the system (generator efficiency η_G, mechanical efficiency η_m, external glands losses ζ_n:

$$N_{el} = \eta_G \cdot \eta_m \cdot (1 - \zeta_n) \cdot N_T - N_{PG}. \tag{8}$$

The effectiveness of the regenerator (σ_R) is calculated as the relation between the actual temperature increase in the exchanger and the maximum possible increase and is determined by the formula:

$$\sigma_R = \frac{\Delta T_{real}}{\Delta T_{\max}} = \frac{T_6 - T_5}{T_2 - T_5}. \tag{9}$$

The cycle analyses have been performed for 11 different media. The values of the initial vapor parameters have been determined, taking into account the media stability and the maximum cycle efficiency. Although the latest literature provides information about the research of the media at high parameters, e.g., for MDM [31], MM [32], c1cc6 [33], ndodecane [34], R134a [35], n-decane [36], R152, R236fa [37], R245fa [38], HFO-1234ze(E) [39] or titanium tetrachloride [40], the problem of the chemical decomposition of the organic media has not been sufficiently explained. In practice, the plant installation is refilled from time to time with some fresh media. However, to be on the safe side, a margin of 50 °C below the maximum temperature has been assumed while the initial pressure has been limited to 35 MPa (the maximum value for advanced ultra-supercritical steam turbines).

For all the calculated examples of variant 1, the initial parameters (temperature and pressure) and outlet pressure (in the condenser) are presented in Table 1 [41–43]. The pressure in the condenser has been estimated, taking into account the temperature of cooling water equal to 15 °C, but not lower than 3 kPa. The increase in the temperature of the cooling water and the final difference in temperature in the condenser were assumed. Thus, the temperature of the vapor condensation was equal to about 28 °C or more (higher values for the limit of the minimum pressure in the condenser). The efficiencies of particular elements are presented in Table 2 [12,13,18].

Table 1. Initial temperatures, pressures and condenser pressures for different working media for cycles with saturated live vapor and a regenerator for warming up the working fluid.

No.	Fluid	Chemical Formula	Name	Initial Temperature (AD and IZT) T_0 [°C]	Initial Pressure (AD) p_0 [MPa]	Initial Pressure (IZT) p_0 [MPa]	Condenser Pressure (AD and IZT) p_{cond} [MPa]
1	MDM	$C_8H_{24}O_2Si_3$	Octamethyltrisiloxane	686.00	16.00	30.00	0.003
2	D6	$C_{12}H_{36}O_6Si_6$	Dodecamethylcyclohexasiloxane	686.00	9.00	15.00	0.003
3	D4	$C_8H_{24}O_4Si_4$	Octamethylcyclotetrasiloxane	686.00	11.00	21.00	0.003
4	MM	$C_6H_{18}OSi_2$	Hexamethyldisiloxane	686.00	13.00	24.00	0.006
5	R245fa	$C_3H_3F_5$	1,1,1,3,3-pentafluoropropane	335.00	11.00	35.00	0.161
6	Acetone	C_3H_6O	2-propanone	501.00	12.00	35.00	0.034
7	R365mfc	$C_4H_5F_5$	1,1,1,3,3-pentafluorobutane	420.00	13.00	35.00	0.062
8	c1cc6	C_7H_{14}	Methylcyclohexane	570.00	12.00	32.00	0.007
9	c3cc6	C_9H_{18}	N-propylcyclohexane	650.00	12.00	29.00	0.003
10	R1233zd	$C_{11}H_{24}$	Undecane	500.00	17.00	35.00	0.140
11	C11	$C_3H_2ClF_3$	1-chloro-3,3,3-trifluoroprop-1-ene	700.00	13.00	27.00	0.003

Table 2. Assumed values of the efficiencies of particular cycle elements.

Description	Symbol	Value	Unit
Turbine efficiency	η_T	0.85	[−]
Pump efficiency	η_{PG}	0.80	[−]
Mechanical efficiency	η_m	0.98	[−]
External glands losses	ζ_n	0.02	[−]
Generator efficiency	η_G	0.90	[−]
Regenerator efficiency	η_R	0.95	[−]
Pressure drop in vapor generator/regenerator	p_i/p_{i-1}	0.98	[−]

3. Results and Discussion

The interpretations of the calculated cycles with the adiabatic and isothermal turbines are presented in Figures 2–7. As examples of working media, $C_6H_{18}OSi_2$ (MM), C_7H_{14} (c1cc6), C_9H_{18} (c3cc6), $C_8H_{24}O_2Si_3$ (MDM), $C_{11}H_{24}$ (C11) and C_3H_6O (acetone) have been chosen.

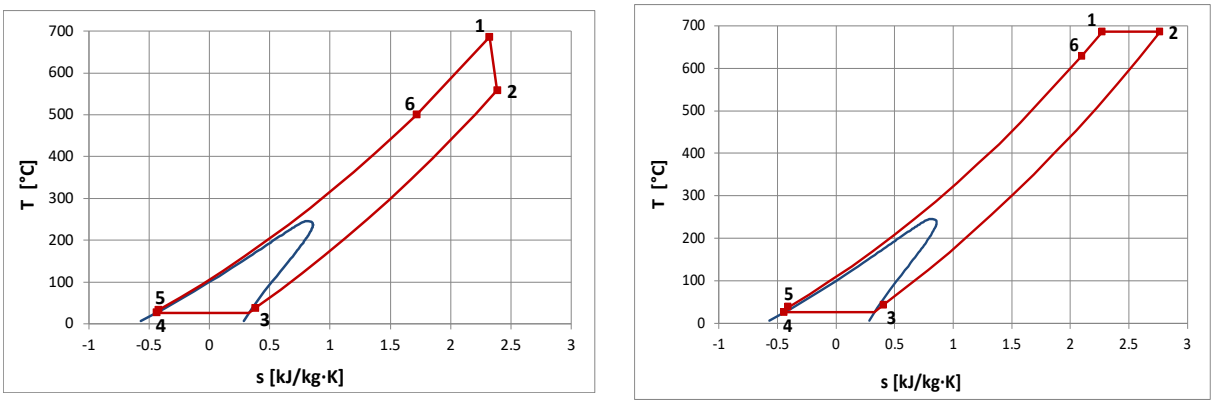

(**a**) (**b**)

Figure 2. Interpretation of cycles with adiabatic (**a**) and isothermal (**b**) expansion (working medium: MM); where: limit line—blue curve and calculated cycle—red line, digits from 1 to 6 are the characteristic points of the analyzed cycle, according to the markings in Figure 1a.

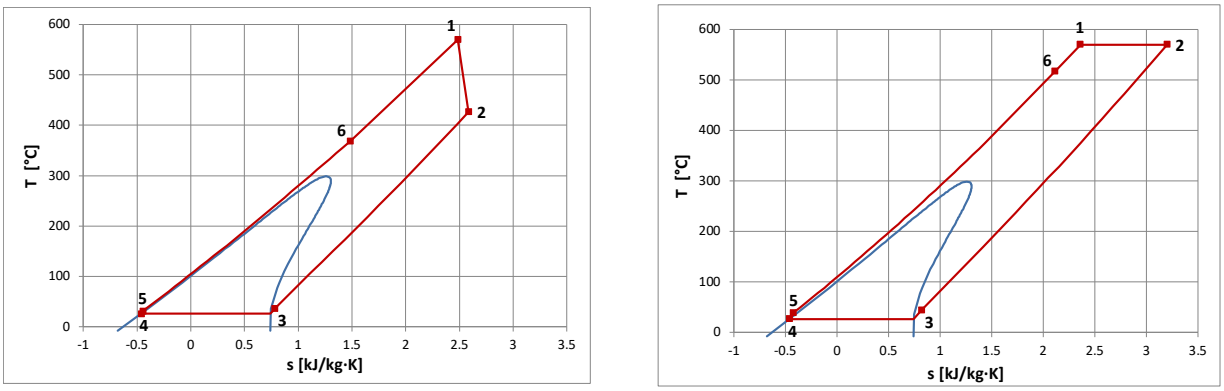

(**a**) (**b**)

Figure 3. Interpretation of cycles with adiabatic (**a**) and isothermal (**b**) expansion (working medium: c1cc6); where: limit line—blue curve and calculated cycle—red line, digits from 1 to 6 are the characteristic points of the analyzed cycle, according to the markings in Figure 1a.

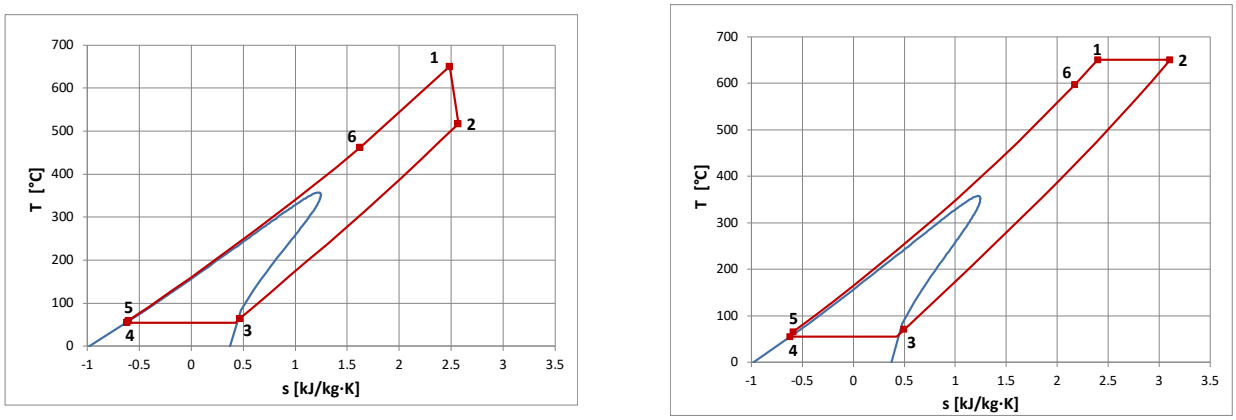

(**a**) (**b**)

Figure 4. Interpretation of cycles with adiabatic (**a**) and isothermal (**b**) expansion (working medium: c3cc6); where: limit line—blue curve and calculated cycle—red line, digits from 1 to 6 are the characteristic points of the analyzed cycle, according to the markings in Figure 1a.

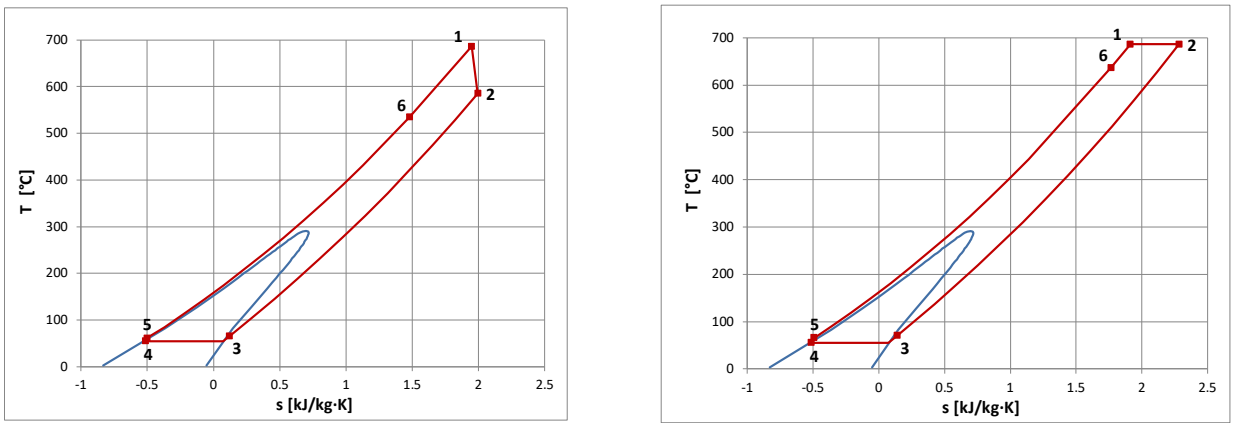

(**a**) (**b**)

Figure 5. Interpretation of cycles with adiabatic (**a**) and isothermal (**b**) expansion (working medium: MDM); where: limit line—blue curve and calculated cycle—red line, digits from 1 to 6 are the characteristic points of the analyzed cycle, according to the markings in Figure 1a.

As can be seen in Figures 2–7, the type of factor has a very large impact on the initial and final values of the parameters at the turbine inlet. The saturation curves for the 11 analyzed factors are very diverse. This affects both the initial temperature (from 335 °C for R245fa to 700 °C for C11) but also the final pressure (from a minimum of 3kPa for MDM, D4, D6, c3cc6 and C11 to 161 kPa for just R245fa). However, in each of the analyzed cases, the application of isothermal expansion also causes, apart from greater work obtained in the turbine, an increase in the amount of heat (area under curves 2–3 in Figures 2–7) that can be recovered in the regenerator—marked as Vb in Figure 1a. Numerical values are presented in Table 3.

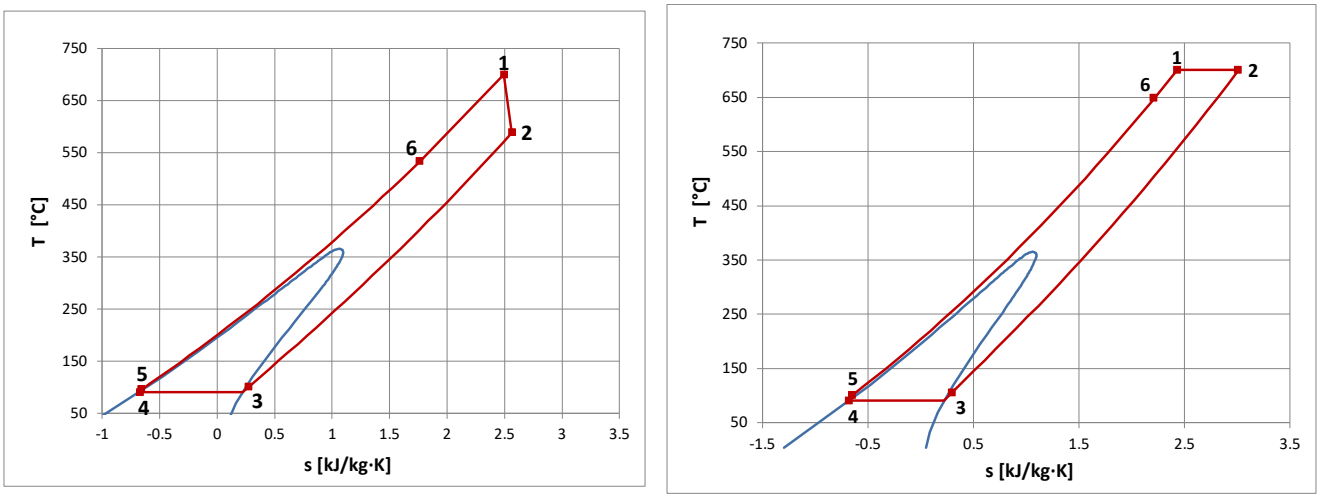

(**a**) (**b**)

Figure 6. Interpretation of cycles with adiabatic (**a**) and isothermal (**b**) expansion (working medium: C11); where: limit line—blue curve and calculated cycle—red line, digits from 1 to 6 are the characteristic points of the analyzed cycle, according to the markings in Figure 1a.

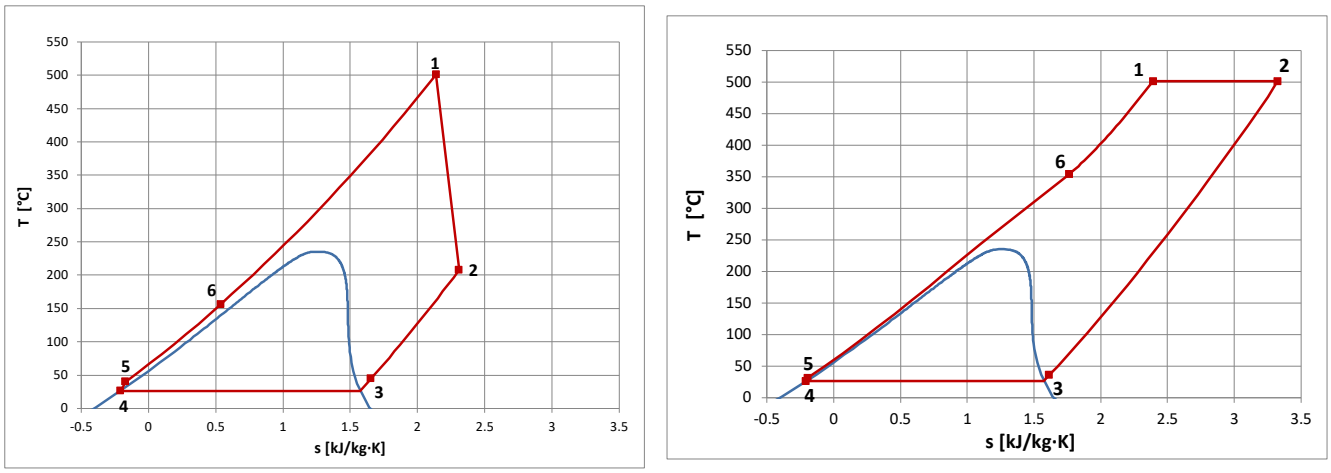

(**a**) (**b**)

Figure 7. Interpretation of cycles with adiabatic (**a**) and isothermal (**b**) expansion (working medium: acetone); where: limit line—blue curve and calculated cycle—red line, digits from 1 to 6 are the characteristic points of the analyzed cycle, according to the markings in Figure 1a.

In the variant with the adiabatic turbine, the smallest efficiency was determined for R245fa (28.7%) and for R365mfc (34%), while the highest values of about 45.3% were found for MM. For isothermal expansion, the smallest efficiency was also found for R245fa (37.3%) and for D6 (41.1%) while the highest efficiency of about 51.7% was obtained for MM. In each case, the efficiency of the cycle with isothermal expansion is remarkably higher than the efficiency of the cycle with adiabatic expansion. The increase in efficiency varies from 8 points for R245fa up to 10 points for acetone. From the above considerations, it follows that the power plants with isothermal turbines (isothermal expansion) are characterized by significantly higher efficiency than the cycles with adiabatic expansion.

The working fluids are characterized by different values of the maximum applicable temperature; thus, it seems that the ratio of the total efficiency to the efficiency of the appropriate Carnot cycle (in the same temperature range) would be more suitable for the assessment of the cycle effectiveness (Figure 8). In this type of analysis, the most

favorable fluids are acetone, c1cc6 and c3cc6, whose efficiency ratio is equal to 0.77. The use of isothermal expansion instead of adiabatic expansion allows the value of this ratio to increase from 9 percentage points for MDM, D6, D4 and MM to 17 percentage points for acetone.

Table 3. Overall efficiency, heat to be recovered in the regenerator and turbine work for adiabatic and isothermal expansions.

No.	Fluid	Adiabatic Expansion	Isothermal Expansion	Adiabatic Expansion	Isothermal Expansion	Adiabatic Expansion	Isothermal Expansion
		Overall Efficiency [−]		Heat [kJ/kg]		Turbine Work [kJ/kg]	
1	MDM	0.4259	0.4837	1089.43	1346.03	224.22	312.92
2	D6	0.3584	0.4106	959.12	1105.07	115.76	156.68
3	D4	0.4047	0.4610	936.43	1140.12	175.67	244.01
4	MM	0.4557	0.5169	1108.86	1440.86	302.22	429.02
5	R245fa	0.2870	0.3728	186.12	329.95	109.61	191.84
6	Acetone	0.3679	0.4714	389.57	894.81	424.99	727.99
7	R365mfc	0.3403	0.4217	309.14	494.82	146.77	239.69
8	c1cc6	0.4286	0.4988	905.00	1369.11	387.34	578.33
9	c3cc6	0.4292	0.4937	1173.13	1624.15	372.95	538.03
10	R1233zd	0.3688	0.4588	289.45	493.89	167.97	272.31
11	C11	0.4067	0.4668	1392.12	1793.38	330.42	466.25

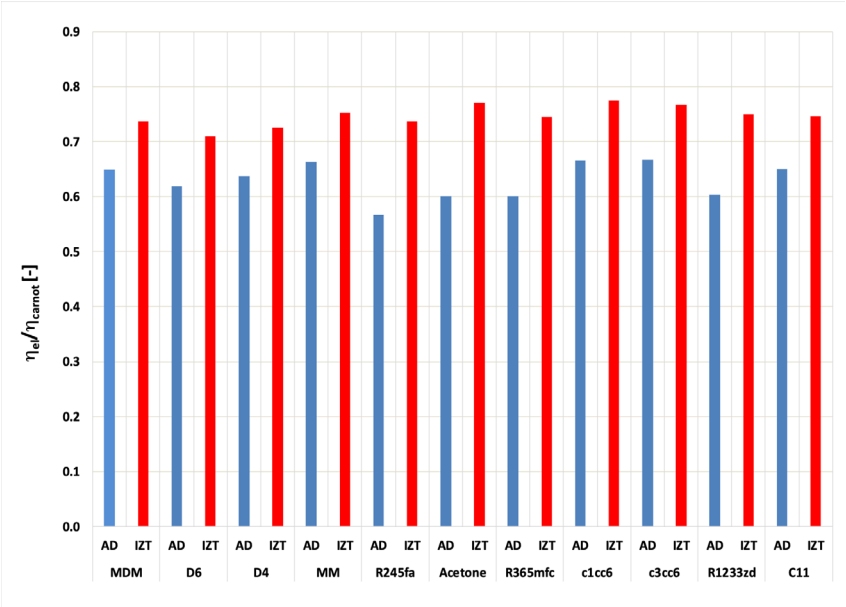

Figure 8. Ratio of the total efficiency to the Carnot cycle efficiency for different working fluids for isothermal (red bars) and adiabatic (blue bars) expansion.

The considerations show that it is possible to design organic power plants of relatively high efficiency even exceeding 50%, which is a very competitive value. It must also be underlined that the increase in initial pressure above the critical value leads to a significant rise in power plant efficiency (at the same upper temperature). In the case of ORC power plants (with a typical adiabatic turbine), the increase in efficiency varies from about two percentage points (acetone, c1cc6 c3cc6) to about six points for the medium R1233zd. For power plants with isothermal turbines, this growth is as high as 3.6 points for c3cc6 up to 10.1 percent points for R1233zd. The comparison of the efficiency for power plants with isothermal and adiabatic expansion is presented in Figure 9 for subcritical live vapor parameters [19] and in Figure 10 for supercritical parameters.

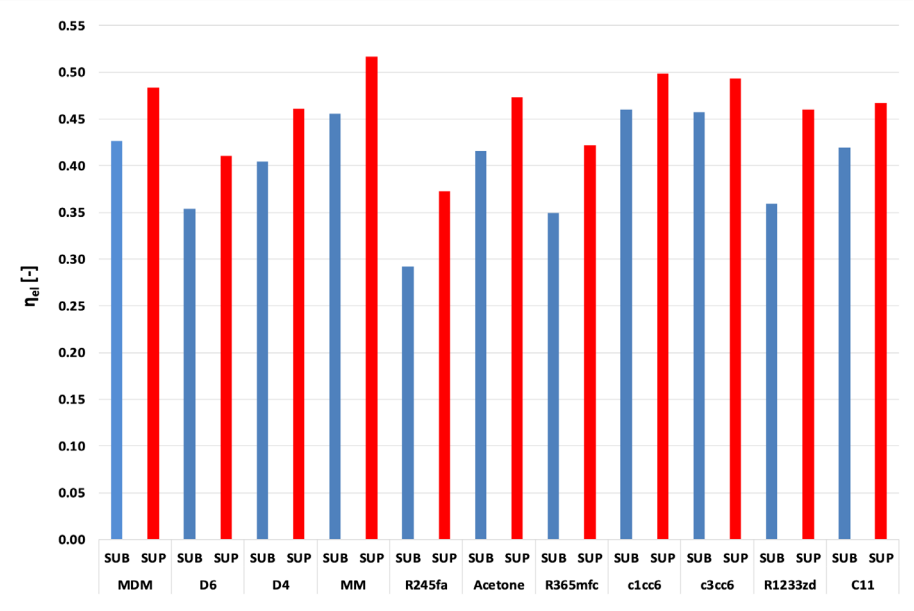

Figure 9. Power plant efficiency for subcritical (blue bars) and supercritical (red bars) parameters (adiabatic turbine).

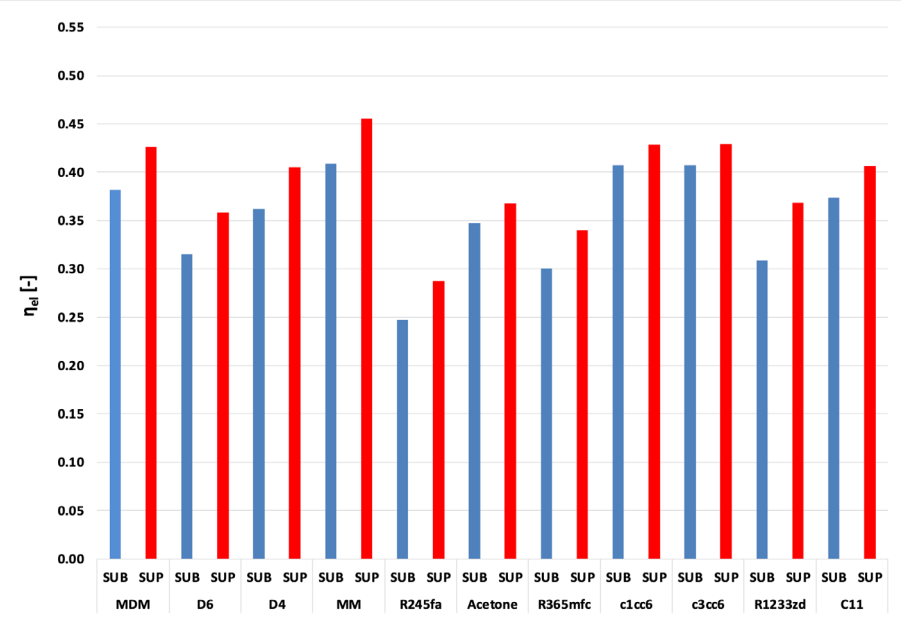

Figure 10. Power plant efficiency for subcritical (blue bars) and supercritical (red bars) parameters (isothermal turbine).

In the case of supercritical parameters, due to a higher value of the initial pressure, we observe higher cycle efficiency than for the power plants with subcritical parameters. The comparison of the optimum value of the initial pressure for subcritical and supercritical parameters is shown in Figure 11 for isothermal expansion and in Figure 12 for adiabatic turbines. The difference in the optimum initial pressure can reach several MPa and, sometimes, even more than 30 MPa (R365mfc).

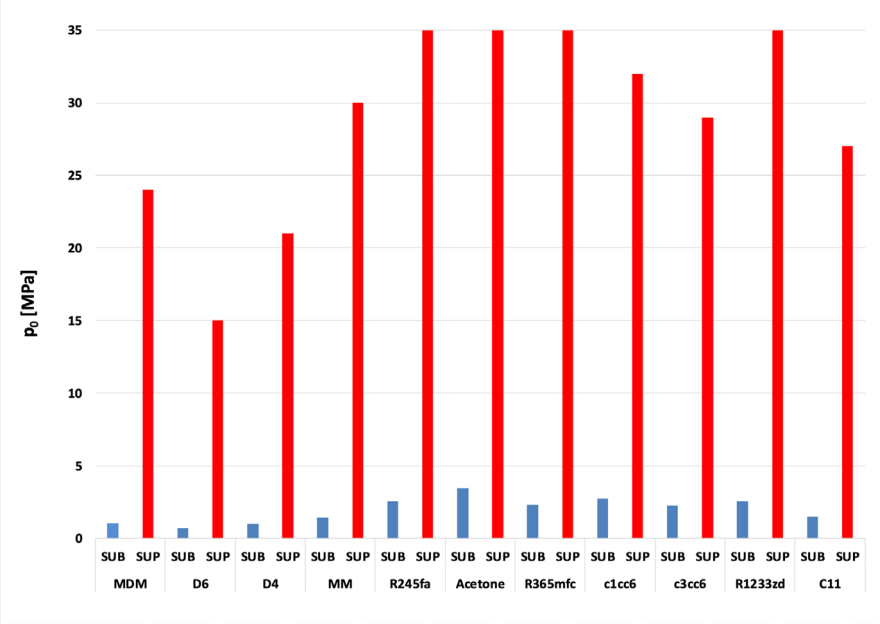

Figure 11. Initial pressures for subcritical (blue bars) and supercritical (red bars) parameters (isothermal turbine).

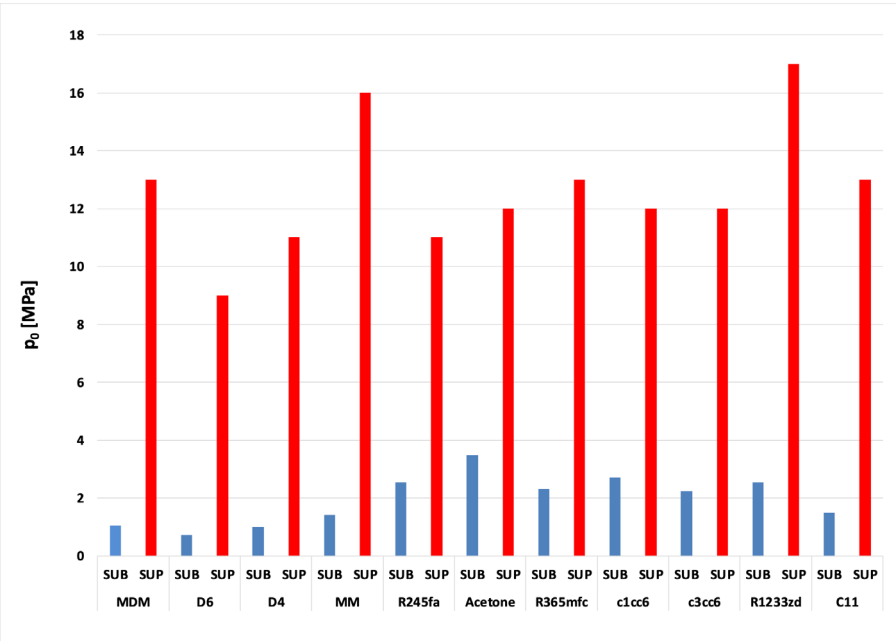

Figure 12. Initial pressures for subcritical (blue bars) and supercritical (red bars) parameters (adiabatic turbine).

The ratio of the total efficiency to the Carnot cycle efficiency for subcritical and supercritical parameters is shown in Figure 13 for adiabatic expansion and in Figure 14 for isothermal turbines. The increase in this ratio varies from 3 percentage points for c1cc6 and c3cc6 fluids and supercritical parameters up to 16 percentage points for R245fa and R1233zd fluids and subcritical parameters.

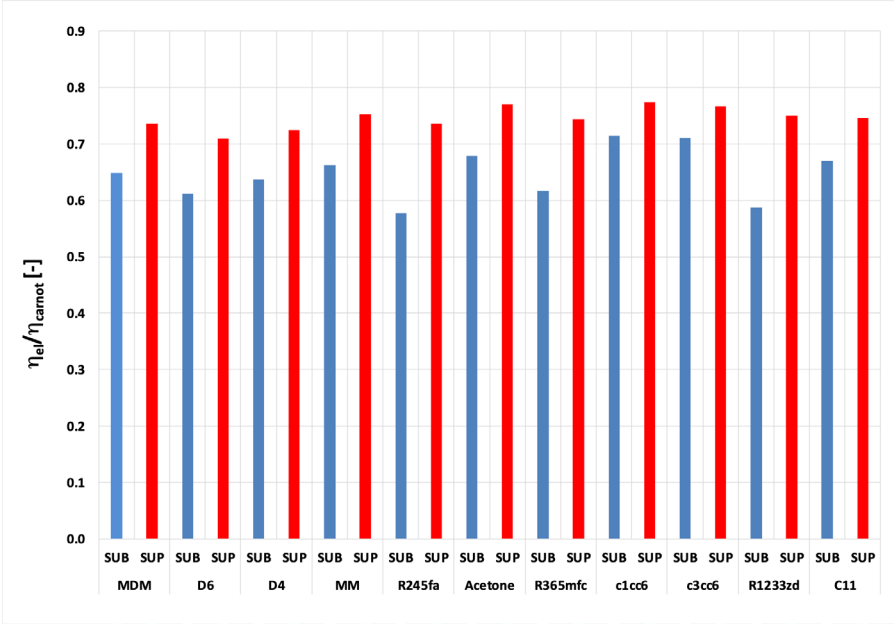

Figure 13. Ratio of the total efficiency to the Carnot cycle efficiency for subcritical (blue bars) and supercritical (red bars) parameters (isothermal turbine).

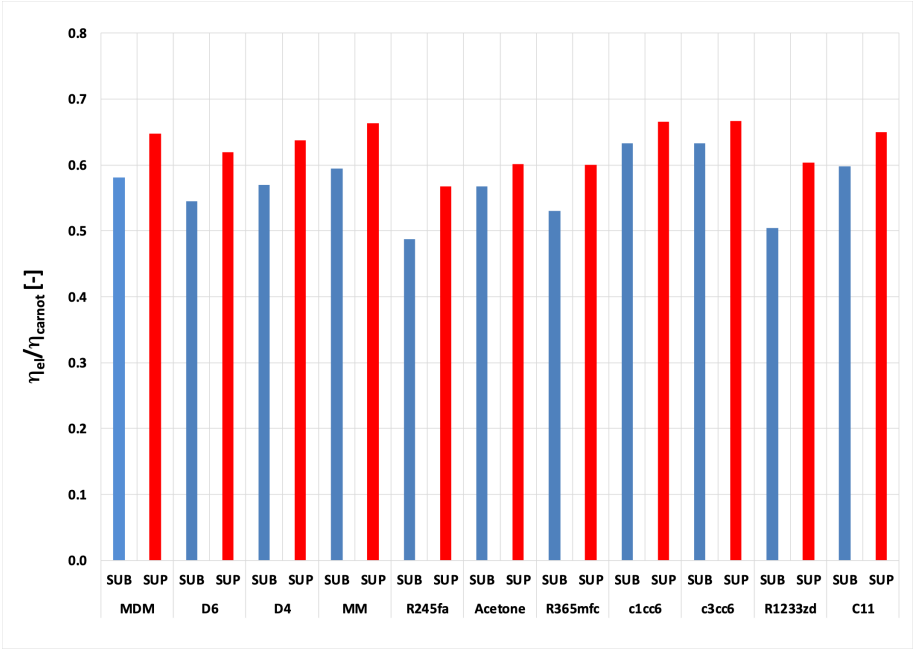

Figure 14. Ratio of the total efficiency to the Carnot cycle efficiency for subcritical (blue bars) and supercritical (red bars) parameters (adiabatic turbine).

4. Conclusions

Nowadays, only simple ORC plants of small output are applied. As a rule, in these units, adiabatic turbines are used to drive an electric generator. The live vapor temperature in these cases is relatively low (<300 °C). The presented analyses have been performed for supercritical parameters of live vapor: high pressures and temperatures up to 700 °C. Furthermore, the thermodynamic cycles of power plants with organic media have been modified, and instead of typical organic Rankine cycles (ORC), organic cycles with isothermal expansion have been proposed and analyzed.

1. It is possible to design organic power plants with relatively high efficiency even exceeding 50% (for MM as a working media at the temperature of 686 °C and pressure p_0 = 13 MPa). In the case of steam power plants, such high efficiencies can be achieved for ultra-supercritical steam parameters (pressures of the order of 30 MPa, temperatures of 600 °C, even above 700 °C, with double interstage superheating and an extensive system of regenerative heaters).
2. The increase in initial pressure above the critical value leads to a significant rise in power plant efficiency (at the same upper temperature). The increase in initial pressure above the critical value causes the increase in efficiency of ORC power plant from about two percentage points (acetone, c1cc6 c3cc6) to about six points for the medium R1233zd for power plants with adiabatic turbines, and for power plants with isothermal turbines, this growth is as high as 3.6 points for c3cc6 up to 10.1 percent points for R1233zd. The values depend on the working media and on their parameters.
3. The efficiency of the cycle with isothermal expansion is visibly higher than the efficiency of the cycle with the adiabatic turbine. The increase in efficiency varies from 8 points for R245fa up to 10 points for acetone.
4. The isothermal expansion and the supercritical parameters of working media can significantly increase the efficiency of ORC power plants by up to 47−51%, which are competitive values characteristic of modern advanced power plants with ultra-supercritical parameters.

Isothermal expansion can be considered as a very effective and significant method of increasing power plant efficiency. Thus, the most important innovation is that instead of a typical adiabatic turbine, an isothermal turbine is applied. These types of power plants with organic media have not been described in the literature so far.

Our team has successfully designed, built and tested an experimental isothermal turbine. The photo of its model and the experimental stand is presented in [19]. Therefore, the obtained results can be of great relevance in future designs.

Author Contributions: Conceptualization, K.K., M.P. and M.R.; methodology, K.K., M.P. and M.R.; formal analysis K.K., M.P. and M.R.; data curation, K.K., M.P. and M.R.; writing—original draft preparation, K.K., M.P. and M.R.; writing—review and editing, K.K., M.P. and M.R.; supervision, K.K. and M.P. All authors have read and agreed to the published version of the manuscript.

Funding: This research received no external funding.

Data Availability Statement: Not applicable.

Conflicts of Interest: The authors declare no conflict of interest. The funders had no role in the design of the study; in the collection, analyses, or interpretation of data; in the writing of the manuscript, and in the decision to publish the results.

Appendix A

Due to the fact that the new concept of the turbine expansion has not been applied yet, the following comments are presented in order to prove that it is possible to design and build flow channels for isothermal turbines.

Isothermal expansion in impulse microturbines with low-boiling-point fluids as the working medium can be achieved in a heated flow channel with an annular or rectangular cross-section. The following numerical nozzle analysis refers to the designed microturbine set. The nozzle heating source is an internal cylindrical heating surface with a diameter of 100 mm and a temperature of 1200 °C. The assumed temperature of the outer wall was estimated to be equal to 1050 °C. The working gas is octamethyltrisiloxane $C_8H_{24}O_2Si$—MDM at a temperature of 300 °C, which ensures the fluid boiling point is exceeded. The inlet and outlet pressures are p_1 = 1.8 MPa and p_2 = 1.1 MPa, respectively. The height of the nozzle outlet correlates with the height of the rotor blades and is equal to 10 mm. The height of the inlet nozzle area equals 74 mm.

The flow in the nozzle was simulated using the ANSYS CFX code. The gas parameters were based on the REFPROP [34]. The heat transfer was defined as total energy including viscous work term. The simulation was performed by means of the SST turbulence model. Multizone body meshing with 28/33 inflation layers with a constant growth rate of 1.2 was applied. The maximum value of the y+ function was 3.67. The meshed body of the nozzle is shown in Figure A1.

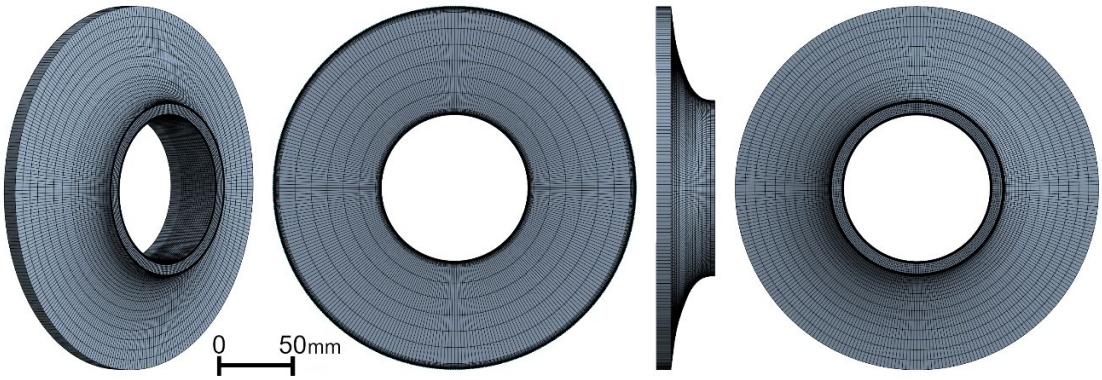

Figure A1. Meshing of the designed nozzle with the annular cross-section.

The total flow channel length is 40 mm. Figure A2 shows the nozzle cross-sectional area and the gas mass flow average temperature as a function of the nozzle length. Figure A3 presents the gas mass flow average velocity and pressure as a function of the nozzle length.

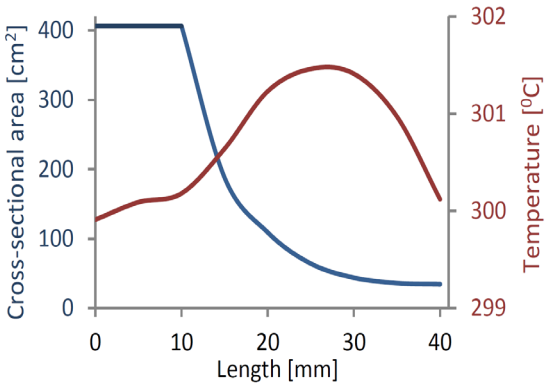

Figure A2. Cross-sectional area and mass flow average gas temperature as a function of nozzle length.

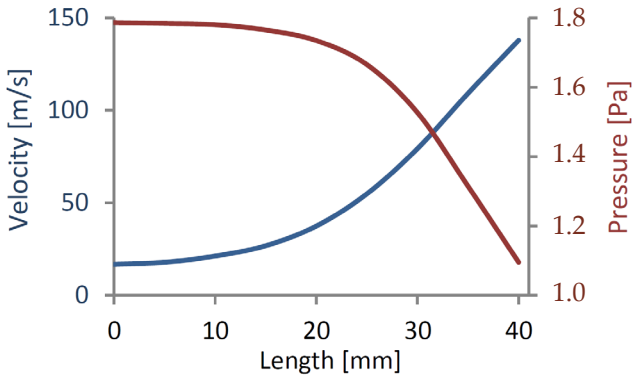

Figure A3. Mass flow average velocity and pressure as a function of nozzle length.

The first 10 mm of the nozzle is an unheated inlet segment that stabilizes the parameters of the working medium. Fluctuations in the gas average temperature during the

flow in the nozzle do not exceed 1.5 °C. The reduction in the cross-sectional area in the inlet section is aimed at increasing the gas velocity and thus limiting the initial rise in its temperature. Despite the great reduction in the cross-sectional area, no flow disturbance was observed.

Figure A4 shows the velocity and temperature distribution of the working medium in the nozzle outlet. The relatively short total length of the flow channel results in uniform temperature distribution and the absence of a boundary layer at the outlet. The elimination of the velocity non-uniformity in the flow can be achieved by designing a symmetrical flow channel taking into account the limitation of the minimum diameter of the radiant tube. The flow parameters are presented in Table A1. The total nozzle length includes the unheated inlet section (of 10 mm).

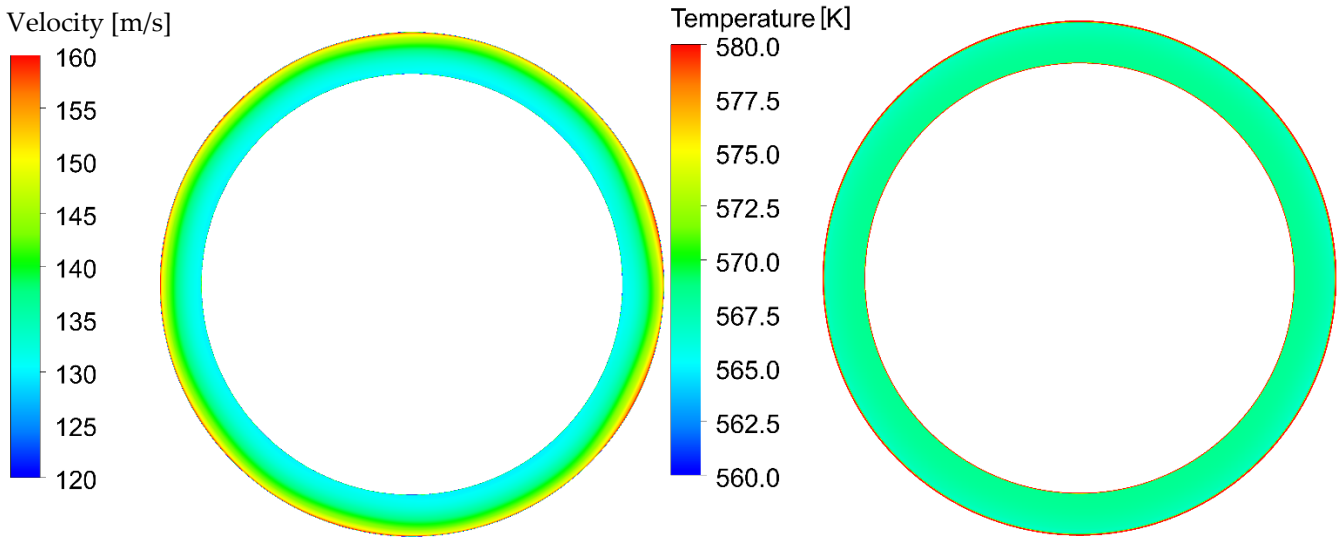

Figure A4. Velocity and temperature distribution at the nozzle outlet.

Table A1. MDM flow parameters—isothermal nozzle with the annular cross—section.

Description	Symbol	Value	Unit
Mass flux	m_p	2.625	[kg/s]
Nozzle inlet pressure	p_1	178.65	[Pa]
Nozzle outlet pressure	p_2	109.52	[Pa]
Nozzle inlet velocity	v_1	16.76	[m/s]
Nozzle outlet velocity	v_2	137.90	[m/s]
Nozzle inlet temperature	T_1	299.91	[°C]
Nozzle outlet temperature	T_2	300.12	[°C]
Non-dimensional wall distance for a wall-bounded flow	y+	3.663	[−]
Total nozzle length	l	40	[mm]

The average outlet velocity in the designed nozzle is close to the theoretical value calculated for the isothermal process (A1):

$$v_2 = \sqrt{2RTln\frac{p_1}{p_2} + {v_1}^2} \quad \text{(A1)}$$

The ratio of the obtained velocity to the theoretical velocity is 0.975. Taking into account the change in the gas enthalpy, the following relation between the energy at the nozzle outlet and at the nozzle inlet can be written in the form (A2):

$$\frac{kineticenergy_{outlet} + staticenthalpy_{outlet}}{kineticenergy_{inlet} + staticenthalpy_{inlet} + wallheatflux} \quad \text{(A2)}$$

Using this formula for the designed nozzle, we receive a result equal to 0.9964. Both these values confirm the minimal influence of the boundary layer on the gas flow in the nozzle.

Thus, the results confirm our assumption that it is possible to design turbine flow channels for isothermal expansion.

References

1. Beith, R. *Small and Micro Combined Heat and Power CHP Systems*; Woodhead Publishing Limited: Cambridge, UK, 2011.
2. Quoilin, S.; Declaye, S.; Tchanche, B.F.; Lemort, V. Thermo-economic optimization of waste heat recovery Organic Rankine Cycles. *Appl. Therm. Eng.* **2011**, *31*, 2885–2893. [CrossRef]
3. Lecompte, S.; Huisseune, H.; Van den Broek, M.; Vanslambrouck, B.; DePaepe, M. Review of organic Rankine cycle (ORC) architectures for waste heat recovery. *Renew. Sustain. Energy Rev.* **2015**, *47*, 448–461. [CrossRef]
4. Zhao, Y.; Liu, G.; Li, L.; Yang, Q.; Tang, B.; Liu, Y. Expansion devices for organic Rankine cycle (ORC) using in low temperature heat recovery: A review. *Energy Convers. Manag.* **2019**, *199*, 111944. [CrossRef]
5. Kermani, M.; Wallerand, A.S.; Kantor, I.D.; Maréchal, F. Generic superstructure synthesis of organic Rankine cycles for waste heat recovery in industrial processes. *Appl. Energy* **2018**, *212*, 1203–1225. [CrossRef]
6. Da Silva, J.A.M.; Seifert, V.; de Morais, V.O.B.; Tsolakis, A.; Herreros, J.; Torres, E. Exergy evaluation and ORC use as an alternative for efficiency improvement in a CI-engine power plant. *Sustain. Energy Technol. Assess.* **2018**, *30*, 216–223. [CrossRef]
7. Li, T.; Meng, N.; Liu, J.; Zhu, J.; Kong, X. Thermodynamic and economic evaluation of the organic Rankine cycle(ORC) and two-stage series organic Rankine cycle (TSORC) for flue gas heat recovery. *Energy Convers. Manag.* **2019**, *183*, 816–829. [CrossRef]
8. Altun, A.F.; Kilic, M. Thermodynamic performance evaluation of a geothermal ORC power plant. *Renew. Energy* **2020**, *148*, 261–274. [CrossRef]
9. Tartiere, T.; Astolfi, M. A World Overview of the Organic Rankine Cycle Market. *Energy Procedia* **2017**, *129*, 2–9. [CrossRef]
10. Piwowarski, M. Design analysis of ORC micro-turbines making use of thermal energy of oceans. *Pol. Marit. Res.* **2013**, *20*, 48–60. [CrossRef]
11. Quoilin, S.; Lemort, V. Technological and Economical Survey of Organic Rankine Cycle Systems. In Proceedings of the 5th European Conference Economics and Management of Energy in Industry, Vilamoura, Portugal, 14–17 April 2009.
12. Kosowski, K.; Piwowarski, M.; Stepien, R.; Włodarski, W. Design and investigations of the ethanol microturbine. *Arch. Thermodyn.* **2018**, *39*, 41–54.
13. Landelle, A.; Tauveron, N.; Haberschill, P.; Revellin, R.; Colasson, S. Organic Rankine cycle design and performance comparison based on experimental database. *Appl. Energy* **2017**, *204*, 1172–1187. [CrossRef]
14. Colonna, P.; Nannan, N.R.; Guardone, A.; Lemmon, E.W. Multiparameter equations of state for selected siloxanes. *Fluid Phase Equilibria* **2006**, *244*, 193–211. [CrossRef]
15. Tchanche, B.F.; Lambrinos, G.; Frangoudakis, A.; Papadakis, G. Low-grade heat conversion into power using organic Rankine cycles—A review of various applications. *Renew. Sustain. Energy Rev.* **2011**, *15*, 3963–3979. [CrossRef]
16. Stępniak, D.; Piwowarski, M. Analyzing selection of low-temperature medium for cogeneration micro power plant. *Pol. J. Environ. Stud.* **2014**, *23*, 1417–1421.
17. Kosowski, K.; Piwowarski, M. Subcritical Thermodynamic Cycles with Organic Medium and Isothermal Expansion. *Energies* **2020**, *13*, 4340. [CrossRef]
18. Vescovo, R.; Spagnoli, E. High Temperature ORC Systems. *Energy Procedia* **2017**, *129*, 82–89. [CrossRef]
19. Piwowarski, M.; Kosowski, K. Advanced Turbine Cycles with Organic Media. *Energies* **2020**, *13*, 1327. [CrossRef]
20. Braimakis, K.; Karellas, S. Energetic optimization of regenerative Organic Rankine Cycle (ORC) configurations. *Energy Convers. Manag.* **2018**, *159*, 353–370. [CrossRef]
21. Abam, F.I.; Ekwe, E.B.; Effiom, S.O.; Ndukwu, M.C.; Briggs, T.A.; Kadurumba, C.H. Optimum exergetic performance parameters and thermo-sustainability indicators of low-temperature modified organic Rankine cycles (ORCs). *Sustain. Energy Technol. Assess.* **2018**, *30*, 91–104. [CrossRef]
22. Imran, M.; Park, B.S.; Kim, H.J.; Lee, D.H.; Usman, M.; Heo, M. Thermo-economic optimization of Regenerative Organic Rankine Cycle for waste heat recovery applications. *Energy Convers. Manag.* **2014**, *87*, 107–118. [CrossRef]
23. Li, T.; Zhu, J.; Hu, K.; Kang, Z.; Zhang, W. Implementation of PDORC (parallel double-evaporator organic Rankine cycle) to enhance power output in oilfield. *Energy* **2014**, *68*, 680–687. [CrossRef]
24. Hanafi, A.S.; Mostafa, G.M.; Fathy, A.; Waheed, A. Thermo-Economic Analysis of Combined Cycle MED-TVC Desalination System. *Energy Procedia* **2015**, *75*, 1005–1020. [CrossRef]
25. Senary, K.; Hegazy, E.; Tawfik, A.A.; Hasan, A. A Evolution and Trends in LNGC Propulsion Systems. *Port Said Eng. Res. J.* **2016**, *20*, 101–108. [CrossRef]
26. Vetter, C.; Wiemer, H.-J.; Kuhn, D. Comparison of sub- and supercritical Organic Rankine Cycles for power generation from low-temperature/low-enthalpy geothermal wells, considering specific net power output and efficiency. *Appl. Therm. Eng.* **2013**, *51*, 871–879. [CrossRef]
27. Xia, X.X.; Qi, W.Z.; Hua, H.Y.; Jun, Z.N. A novel comprehensive evaluation methodology of organic Rankine cycle for parameters design and working fluid selection. *Appl. Therm. Eng.* **2018**, *143*, 283292. [CrossRef]

28. Cicconardi, S.P.; Jannelli, E.; Perna, A.; Spazzafumo, G. Parametric analysis of a steam cycle with a quasi-isothermal expansion. International. *J. Hydrog. Energy* **2001**, *26*, 275–279. [CrossRef]
29. Zhang, X.; Xu, Y.; Zhou, X.; Zhang, Y.; Li, W.; Zuo, Z.; Guo, H.; Huang, Y.; Chen, H. A near-isothermal expander for isothermal compressed air energy storage system. *Appl. Energy* **2018**, *225*, 955–964. [CrossRef]
30. Lemmon, E.; Huber, M.; McLinden, M. *NIST Standard Reference Database 23: Reference Fluid Thermodynamic and Transport Properties-REFPROP*; Version 9.0 Edition; National Institute of Standards and Technology, Standard Reference Data Program: Gaithersburg, MD, USA, 2010.
31. Keulen, L.; Landolina, C.; Spinelli, A.; Iora, P.; Invernizzi, C. Design and commissioning of a thermal stability test-rig for mixtures as working fluids for ORC applications. *Energy Procedia* **2017**, *129*, 176–183. [CrossRef]
32. Xu, G.; Fu, J.; Quan, Y.; Wen, J.; Dong, B. Experimental investigation on heat transfer characteristics of hexamethyldisiloxane (MM) at supercritical pressures for medium/high temperature ORC applications. *Int. J. Heat Mass Transf.* **2020**, *156*, 119852. [CrossRef]
33. Bounaceur, R.; Burklé-Vitzthum, V.; Marquaire, P.-M.; Fusetti, L. Mechanistic modeling of the thermal cracking of methylcyclohexane nearatmospheric pressure, from 523 to 1273 K: Identification of aromatization pathways. *J. Anal. Appl. Pyrolysis* **2013**, *103*, 240–254. [CrossRef]
34. Herbinet, O.; Marquaire, P.-M.; Battin-Leclerc, F.; Fournet, R. Thermal decomposition of n-dodecane: Experiments and kinetic modelling. *J. Anal. Appl. Pyrolysis* **2007**, *78*, 419–429. [CrossRef]
35. Invernizzi, C.M.; Iora, P.; Preißinger, M.; Manzolini, G. HFOs as substitute for R-134a as working fluids in ORC power plants: A thermodynamic assessment and thermal stability analysis. *Appl. Therm. Eng.* **2016**, *103*, 790–797. [CrossRef]
36. Wang, Y.; Zhao, Y.; Liang, C.; Chen, Y.; Zhang, Q.; Li, X.Y. Molecular-level modeling investigation of n-decane pyrolysis at high temperature. *J. Anal. Appl. Pyrolysis* **2017**, *128*, 412–422. [CrossRef]
37. Dai, X.; Shi, L.; An, Q.; Qian, W. Thermal stability of some hydrofluorocarbons as supercritical ORCs working fluids. *Appl. Therm. Eng.* **2018**, *128*, 1095–1101. [CrossRef]
38. Kong, R.; Deethayat, T.; Asanakham, A.; Vorayos, N.; Kiatsiriroat, T. Thermodynamic performance analysis of a R245fa organic Rankine cycle (ORC) with different kinds of heat sources at evaporator. *Case Stud. Therm. Eng.* **2019**, *13*, 100385. [CrossRef]
39. Irriyantoa, M.Z.; Limb, H.-S.; Choib, B.-S.; Myinta, A.A.; Kim, J. Thermal stability and decomposition behavior of HFO-1234ze(E) as aworking fluid in the supercritical organic Rankine cycle. *J. Supercrit. Fluids* **2019**, *154*, 104602. [CrossRef]
40. Invernizzi, C.M.; Iora, P.; Bonalumi, D.; Macchi, E.; Roberto, R.; Caldera, M. Titanium tetrachloride as novel working fluid for high temperature Rankine Cycles: Thermodynamic analysis and experimental assessment of the thermal stability. *Appl. Therm. Eng.* **2016**, *107*, 21–27. [CrossRef]
41. Set of Product's Card of Chempur Poland Ltd. Available online: http://en.chempur.pl (accessed on 22 August 2020).
42. Set of Product's Card of Sigma-Aldrich Ltd. Available online: https://www.sigmaaldrich.com (accessed on 22 August 2020).
43. Set of Product's Card of SCHIESSL Poland Ltd. Available online: https://www.schiessl.pl/en (accessed on 22 August 2020).